electronic reprint

Journal of
Applied Crystallography
ISSN 0021-8898

Pore characteristics and water absorption in a synthetic smectite clay

Kenneth D. Knudsen, Jon Otto Fossum, Geir Helgesen and Vegard Bergaplass

Pore characteristics and water absorption in a synthetic smectite clay

Kenneth D. Knudsen,[a]* Jon Otto Fossum,[b] Geir Helgesen[a] and Vegard Bergaplass[b]

[a]*Institute for Energy Technology, POB 40, N-2027 Kjeller, Norway,* [b]*The Norwegian University of Science and Technology, NTNU, Department of Physics, N-7491 Trondheim, Norway. E-mail: knudsen@ife.no*

Information on size and shape of pores in layered silicates can be obtained via analysis of the relative scattered intensity for different scattering vectors. In this study the small-angle neutron scattering technique was used to investigate the synthetic clay Na-fluorohectorite. The anisotropically shaped pores showed an average correlation length ratio of about 1:2 between the direction of sedimentation and the direction perpendicular to this. The absorption of water, which can be controlled via the temperature and humidity of the surrounding air, consists both in the intercalation of water molecules between the clay platelets and the filling of the mesopores between the platelet stacks.

Keywords: clay; **small-angle neutron scattering**; **water absorption.**

1. Introduction

Platelet structures made up of silicates (clays) are traditional materials with a number of important applications (Velde, 1992), e.g. in pottery, as waste barriers or as inexpensive filler material. Clays may be considered physical colloids in the form of aqueous suspensions made up of plate-like layered silicates as primary particles. Dehydrated clays may, on the other hand, be viewed as intercalation compounds (Solin, 1997) within the general context of "nano sandwiches". All dehydrated clays are based on a layered silicate meso-structure. The so-called 2:1 clays (or smectites) thus consist of $\sim$1 nm thick and charged (negative surface charge and a smaller positive edge charge) meso sheets, which in the dehydrated state stack (like decks of cards) by sharing charge-compensating cations. The 1 nm thick sheet may be broken down into three atomic layers, i.e. generally one metal hydroxide layer sandwiched in between two identical silicon tetrahedral oxide layers. In general the clay particles have a high aspect ratio, and sedimentation taking place in a dispersion of clay platelets will induce a preferred orientation, with the platelets lying predominantly perpendicular to the axis of applied hydrostatic pressure.

Clays, as well as some other materials, e.g. carbon fibres or ceramic membranes, have been shown to contain oriented pores in the meso-range (Ramsay, 1998). For these materials, unique directional information can be obtained by combining small-angle X-ray or neutron scattering (SAXS/SANS) with two-dimensional detection.

In the present work small-angle neutron scattering has been employed to obtain information about the synthetic clay X-fluorohectorite, with chemical formula X_y-$(Mg_{3-y}Li_y)Si_4O_{10}F_2$, where X is an exchangeable cation. In this particular case the cation was Na^+. The fluorohectorite is polydisperse, with a platelet diameter ranging from several nm all the way up to about 1 μm. When the sample is in the dissolved state, the polydispersity causes an interesting macroscopic gravity-induced phase separation, where as many as four different phases have been observed to exist simultaneously in the same sample tube (DiMasi *et al.*, 2001).

In the present study samples were prepared from suspension to obtain dehydrated samples by applying hydrostatic pressure (up to 26 MPa). With these dehydrated samples as starting material, the effect of varying temperature and water saturation was studied.

2. Experimental

The small-angle neutron scattering measurements were performed at the SANS installation (beam port 2) at the IFE reactor at Kjeller. A liquid nitrogen cooled 15 cm long Be-filter is installed in the beam path in order to remove fast neutrons (cut-off at λ = 4 Å, λ = wavelength), and an additional 15 cm Bi-filter removes the gamma radiation. The wavelength was set by means of a velocity selector (Dornier), using a high FWHM for the transmitted beam ($\Delta\lambda/\lambda$=20 %), and maximized flux on the sample. The beam divergence was set by an input collimator (18.4 or 12.2 mm diameter) located 2.2 m from the sample, together with a sample collimator which was fixed to 4.9 mm. The neutron detector was a 128x128 pixel, 59 cm active diameter, ^{3}He-filled RISØ-type detector, which is mounted on rails inside an evacuated detector chamber. The distance was varied from 1.0 m to 3.4 m and the wavelength between 5.1 Å and 10.2 Å, giving a q-range from 0.008 to 0.3 Å^{-1} (where $q = 4\pi sin\theta/\lambda$, with θ = half the scattering angle).

The samples were based on synthetic sodium fluorohectorite (Corning Inc., New York). First the fluorohectorite powder was dissolved in deionized water and stirred for several days. Thereafter an ion exchange method was used, adding Na^+ in the form of NaCl, and in an amount of about 10 times the interlayer charge. The amount of salt needed was calculated from values given in Kaviratna *et al.* (1996). After stirring for 2 days we obtained a two-phase system from which the supernatant was removed. The resulting part was then placed in dialysis membranes, and excess ions were removed by dialysis, exchanging the deionized water every 2 days. A check of this procedure was made by adding $AgNO_3$ to the system to detect possible Cl^- ions, which would precipitate as insoluble AgCl. The suspensions of sodium fluorohectorite (NaFH) were thereafter heat pressed at 393 K (120 °C) by exerting mechanical force onto a disc shaped sample volume (Fig. 1*a*). The load used was 10^4 kg, giving a pressure of 26 MPa (260 bar). The final result is a smectite dehydrated clay (Fig. 1*b*) where the clay platelets (1 nm thick) are stacked with preferential orientation such that the main platelet direction is normal to the axis of compression.

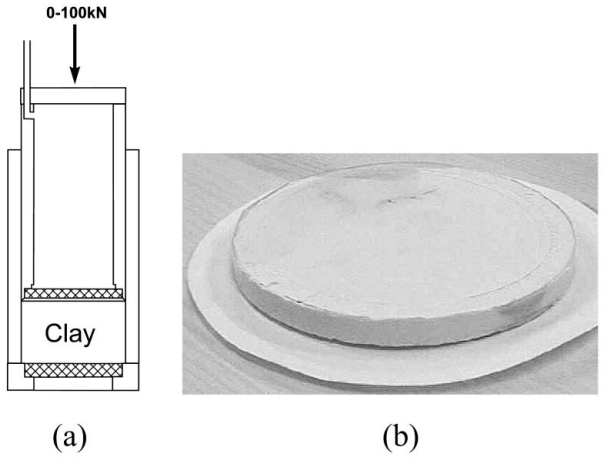

Figure 1
(*a*) The press used to make the dehydrated clay samples (simplified schematic). (*b*) A fluorohectorite sample after leaving the clay press and before being cut for the experiment.

The samples were cut in thin slices (1-2 mm) in order to avoid high neutron absorption and corresponding multiple scattering, placed on a

copper-base for good thermal contact and mounted in the sample cell. The temperature and humidity were controlled by means of a custom-made portable setup that includes the small closed cell containing the sample, as shown in Fig. 2.

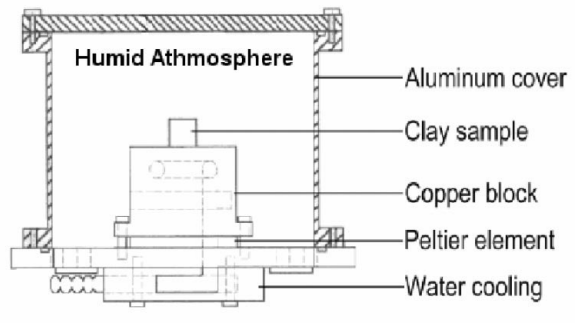

Figure 2
The cell that allows for temperature- and humidity-control of the sample. The housing is made of 2 mm thick aluminium, which absorbs only a small amount of the neutrons at 5 Å. The circuit for humidity control is not shown.

The cell is supplied with tubing where air circulates via a chamber in which the humidity is controlled by means of a saturated salt solution (K_2SO_4 for 97% relative humidity). Heating and cooling is performed by means of an integrated resistance element and a Peltier element, respectively. The setup of the sample with respect to the neutron beam is shown in Fig. 3.

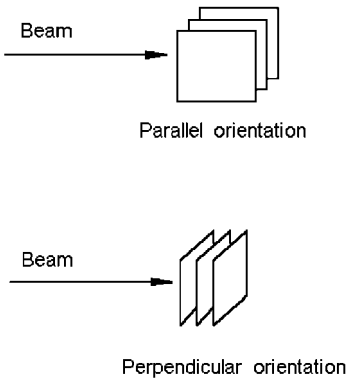

Figure 3
Two different orientations of the sample with respect to the neutron beam used in the experiments. The sample surface is either such that the main platelet direction is perpendicular to the beam, or parallel to the beam.

Standard reductions on the scattering data were performed by incorporating data collected on empty beam (no sample), and blocked-beam background. The data were put on an absolute scale by calculating the normalized scattered intensity from direct beam measurements (Wignall & Bates, 1987).

3. Pore structure and water absorption

¿From knowledge of the specific weight of the sodium fluorohectorite (2.8 g/cm^3, Kaviratna *et al.*, 1996), combined with accurate volume/weight measurements of the samples after they had been heated (in order to remove water), the samples used in this study were found to have a porosity (pore volume to total volume in the dried-out state) of 41%. From X-ray studies (da Silva *et al.*, 2002) it was found that the clay platelets, each about 1 nm thick, tend to stack on top of each other (like a deck of cards) to contain on the average about 100 platelets, giving a typical total height of about 0.1 μm. The lateral dimensions of such a stack are larger, atomic force microscopy data give values up to as much as 10 μm (Kaviratna *et al.*, 1996; Fossum, 1999). This means that even when individual platelets gather into stacks, the resulting "grain" will actually be like a thin disk, where the lateral dimensions may be as much as 100 times the disk thickness. However, the fluorohectorite is polydisperse with a wide distribution in lateral sizes, so that this ratio is not fixed, and may be considerably lower for other grains.

The way the stacks organize with respect to one another during sedimentation and drying (with applied external pressure), may induce the creation of nano- or mesopores with anisotropic structure. One could imagine the pores being flattened in the direction of sedimentation, creating pores with oblate ellipsoidal shape in a simplified picture, and with an anisotropy possibly dependent on the external pressure exerted during sedimentation and drying of the sample (Knudsen *et al.*, 2003).

We have studied the small-angle scattering signal from fluorohectorite to gain information on the organization of this porous structure on length scales larger than that corresponding to the thickness of individual platelets. Of particular interest are the pores that may exist between the different grains of clay. When the clay platelets stack on top of each other, they create a one-dimensional lattice, with a certain repeating distance d in the stacking [001] direction. This distance, which is slightly larger than 1 nm, corresponds to the thickness of a clay platelet plus that of the layer of intercalated ions and water. When an X-ray beam is directed towards a properly oriented sample, this stacking will cause diffraction (Bragg) peaks, and the broadening of these peaks with respect to those of a reference sample can be used to obtain information about strain or stacking faults, i.e. variations in the repeating distance d. Synchrotron X-ray data based on this procedure (da Silva *et al.*, 2002) show deformations (strain) on the order of $\Delta d/d$=1-5x10^{-3}, and such a value would correspond to only very low stacking-fault densities, i.e. nearly perfect (in one dimension) stacking of the platelets on top of each other. However, one cannot exclude possible fracture of the end section of clay platelets, as this would not affect the strain values mentioned above, but only appear as a contribution to the rocking curve for Bragg scattering in X-ray experiments. Such fracture could create nanopores (open or closed) that would also contribute to the scattering we observe in the present SANS data, i.e. in addition to the scattering due to the pores that exist between the different grains. Considering the high porosity of these clay systems (above 40%), combined with the observations of 0.1 μm thick grains, also larger pores, comparable to the size of a grain, are likely to be present between the different grains of clay. However, these large pores are not probed directly by the SANS technique.

3.1. Sample in perpendicular orientation

Fig. 4(*a*) shows a SANS pattern collected for a dehydrated fluorohectorite sample when placed such that the clay platelets are perpendicular to the beam (see Fig. 3, lower part). The scattering produced in this situation probes structures in the plane normal to the axis of compression of the sample. The scattering is isotropic, showing that the scatterers have a symmetric shape as seen with a neutron probe looking in the same direction as the axis of compression.

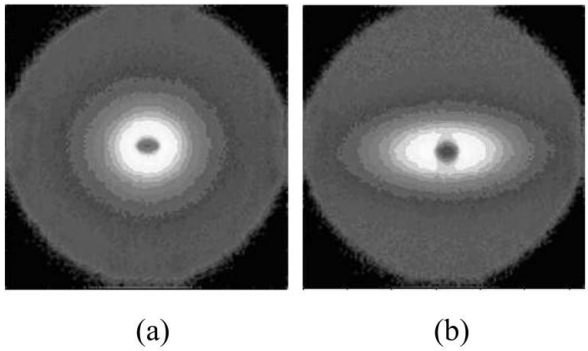

Figure 4
(*a*) Small-angle signal from fluorohectorite with main platelet orientation **perpendicular** to the beam, showing an isotropic signal in the detector plane. (*b*) Small-angle signal from fluorohectorite with main platelet orientation **parallel** to the beam, showing anisotropy with excess intensity in the equatorial plane.

3.2. Sample in parallel orientation

Fig. 4(*b*) shows a SANS pattern collected for a fluorohectorite sample when placed such that the clay platelets are parallel to the beam (Fig. 3, upper part). The scattering produced in this situation probes structural features both in the direction of axial compression and in the plane normal to this direction. The anisotropy of the signal is an indication of non-symmetric scatterers that are anisotropically oriented in the sample. The observed behavior can be explained by imagining the scatterers as mesopores that are flattened in the direction normal to the platelet orientation, i.e. in the same direction as the external pressure applied during sample preparation. When the sample is placed in the parallel orientation, the neutron probe will see the pores from the side, and therefore as something like thin disks with the long axis oriented vertically with respect to the laboratory system. The fact that the signal was isotropic (Fig. 4*a*) when the sample was placed in the perpendicular orientation supports the argument that the pores are flattened only in the direction of the external pressure, with no in-plane asymmetry, so that they will look on average like circular scatterers in the perpendicular orientation.

For a random two-phase system (e.g. void inhomogeneities in a matrix) it is in principle possible to use the Debye-model (Debye & Bueche, 1949; Debye *et al.*, 1957) to define a characteristic inhomogeneity (correlation) length ξ via the relation $I(q) = k(1+\xi^2 q^2)^{-2}$, where k is a numerical constant. The system investigated in the present study is not random, due to correlations between size and orientation, but one may then introduce a two-dimensional Debye-model (Hall *et al.*, 1983) where scattering for a given q-vector depends on azimuthal position on the detector. We employ this model to our asymmetric data by introducing different correlation lengths for the data in the horizontal direction (ξ_1) and the vertical direction (ξ_2).

By plotting $I^{-1/2}$ vs. q^2 in the horizontal and vertical scattering direction, based on integration along those directions in the detector plane, one expects a straight line with slope equal to $\xi^2 k^{-1/2}$ and an intercept at the ordinate axis equal to $k^{-1/2}$. Thus, it is possible to determine the coefficients ξ_1 and ξ_2 via ξ=(slope/intercept)$^{1/2}$.

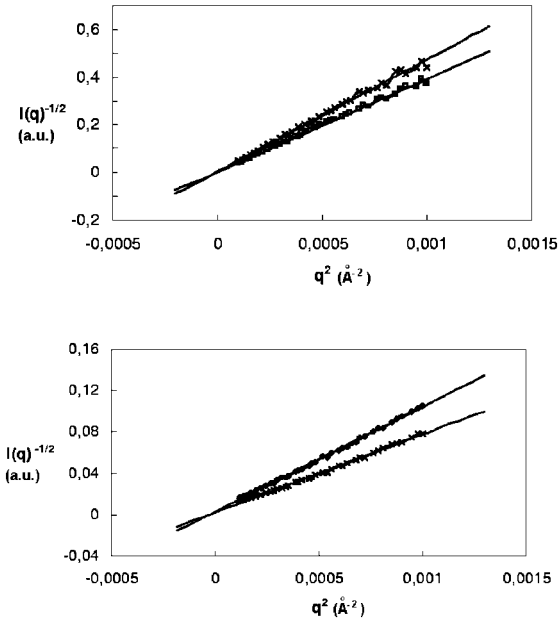

Figure 5
Debye plot for the scattering measured in two different directions on the detector plane, the vertical direction (upper graph) and the horizontal direction (lower graph). The sample was in the parallel orientation (cf. Fig. 3). The q-range used was 0.01-0.032 Å^{-1}. Data were recorded on two different samples prepared with the same experimental protocol.

Fig. 5 shows the corresponding Debye plots for two different samples of sodium fluorohectorite (prepared with the same experimental protocol, as described in section 2). The upper graph corresponds to the vertical scattering direction and the lower graph to the horizontal direction (see Fig. 4*b*).

The average characteristic inhomogeneity lengths obtained via this method are ξ_1=176 Å and ξ_2=383 Å (average of two samples). The ratio of these is a number somewhat less than 0.5. The isointensity lines for the anisotropic scattering signal always showed an elliptical shape for the fluorohectorite system. When measuring the axis ratio of the corresponding ellipse, one finds in all cases an axis ratio of 2.0 ($\pm$0.1). The overall scattered intensity for different q-values is related to the total surface area available for scattering in different directions within the sample. If one obtains anisotropic isointensity lines, the system must therefore have asymmetric and oriented pores, and the axial ratio above should give an estimate of the average deformation of the pores in the sample. The observed deformation ratio of 2:1 corresponds well with the ratio between the Debye inhomogeneity lengths described earlier. The process of sedimentation, compaction and dehydration of the fluorohectorite therefore seems to result in pores that are considerably flattened in the direction parallel to the direction of sedimentation, such that the average compaction ratio of the pores is close to 2:1.

3.3. Variation of humidity and temperature

The use of the specialized cell shown in Fig. 2 made it possible to study the scattering at different combinations of temperature and humidity. As can be seen from Fig. 6, when the humidity is increased and the temperature is reduced, the intensity in the low-q region decreases. On the other hand, when the humidity is reduced and the temperature is increased, there is an increase in the scattered intensity. The curves cross each other at higher q-values and end up at different levels due to the different amounts of water, giving nonequal contributions to inco-

herent scattering.

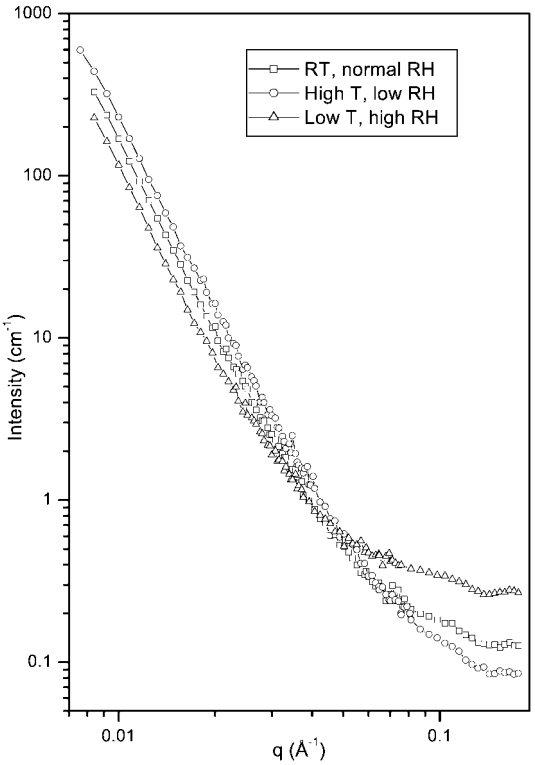

Figure 6
Azimuthally integrated (isotropic) small-angle scattering from Na-fluorohectorite for three different temperatures T and relative humidities (RH). RT = room temperature. The sample was in the perpendicular orientation.

Extraction of the relative intensities (at a specific point, q=0.014 Å^{-1}) for the three cases (*a*) sample with little water (low RH), (*b*) at ambient conditions (normal RH), and (*c*) saturated with water (high RH) gives intensity ratios of 1:0.74:0.51 (dry/normal/wet). An expected value can be calculated by making use of the fact that the intensity ratio will be given by $\Delta\rho_{SLD}{}^2$, where $\Delta\rho_{SLD}$ is the difference in scattering length density between the clay grains and the surroundings. The different situations we consider are: 393 K (120 °C) & RH = 3.7% (dry), 298 K (25 °C) & RH = ambient (normal), and 293 K (20 °C) & RH = 97% (wet). For the calculation the water that is absorbed in between the clay platelets must now be taken into account (for Na-fluorohectorite up to 2 water "layers" can be incorporated). The incorporation of water will change the fluorohectorite scattering length density due to the presence of extra hydrogen and oxygen, but more importantly, because the platelet distance also increases when water enters, the fluorohectorite mass density changes considerably, leading to a significant change in the scattering length density. Table 1 shows calculated scattering length densities for different combinations of fluorohectorite and water.

Table 1
Neutron scattering length densities calculated for different substances relevant for the experiment. *n*WL means number of water layers between the fluorohectorite platelets. NaFH means sodium fluorohectorite.

Substance	ρ_{mass} [g/cm^3]	ρ_{SLD} [10^{-6} Å^{-2}]
H_2O	1.0	-0.56
D_2O	1.1	6.33
NaFH	2.80	4.36
NaFH + 1WL H_2O	2.31	3.33
NaFH + 2WL H_2O	2.02	2.65
NaFH + 1WL D_2O	2.32	4.18

This calculation assumes that when the platelet stacks include one layer of water, a number of 1.2 water molecules is added per 0.6 Na-ion, and that 2.8 water molecules are added per 0.6 Na-ion in the situation with two water layers. It is also assumed that the platelet stacks only expand in the direction parallel to the platelet normal, which is a reasonable assumption for this kind of samples.

If water is contained only within the platelet stacks (air-filled pores), one can calculate from the above table the intensity ratios for the three cases dry/normal/wet, giving the result 1:0.58:0.37. These values differ considerably from those of the experiment (1:0.74:0.51). However, the following model can better explain the experimental data. (*a*) In the high temperature situation (and low humidity) there are zero water layers between the clay platelets, and the pores are filled with air only. (*b*) In the ambient situation there is one water layer incorporated, the pores are air-filled, but can have a thin layer of water on the walls. (*c*) In the situation with lower temperature (and high humidity) there are two water layers incorporated, and the pores are completely filled with water. Using this model, we get an expected intensity ratio of 1:0.81:0.54, which is close to what is observed experimentally.

3.4. Substitution by D_2O

As an initial study of the dynamics of water transport in a wet fluorohectorite system, a H_2O-saturated Na-fluorohectorite sample was exposed to D_2O-filled atmosphere, following the substitution of H_2O by D_2O by measuring the SANS intensity as a function of time. As seen from Fig. 7, the initial rise is quite fast, but the complete substitution is a rather slow process. For this particular sample (2x10x10 mm), about 10 h were necessary to reach the equilibrium state. The intensity change observed here, i.e. a substantial increase as D_2O is incorporated, is unexpected based on the scattering length densities in Table 1. A complete substitution of H_2O by D_2O, including the water between the platelets, would rather be expected to produce a reduction in intensity due to the larger difference in scattering length density (between the clay particles and the pores) when the pores are filled with H_2O than with D_2O. However, an increase can be explained (up to about a factor of 2) if one assumes that D_2O is incorporated in-between the platelets, but that the substitution of the pores is not complete, with a considerable amount of H_2O still adhering to the pore surface. However, we are not able to explain the large increase (factor of about 6) observed here, and further investigations will be needed on this point. One may speculate that in addition to the exchange process, a slow degeneration or restructuring of the internal surface is taking place during the course of the experiment.

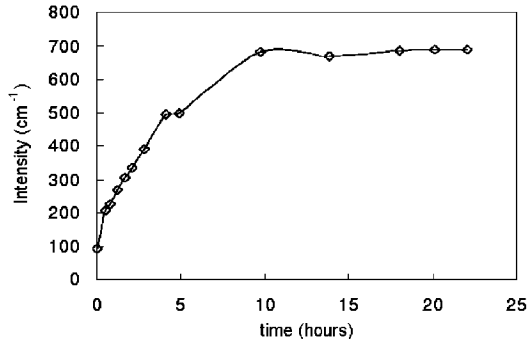

Figure 7
Intensity vs. time in the horizontal scattering direction (measured at q=0.02 Å^{-1}) while substituting H_2O with D_2O. The fluorohectorite sample was in the parallel orientation.

4. Conclusions

The analysis of the relative scattered intensity for different scattering vectors makes it possible to obtain information on both size and shape of pores in layered silicates. An average correlation length ratio of about 1:2 was found between the direction of axial compression and the direction perpendicular to this. The absorption of water can be controlled by means of the temperature and the humidity of the surrounding atmosphere, and in this manner the number of intercalated water layers can be varied between 0 and 2 for the sodium fluorohectorite system. The absorption of water also results in a partial or complete filling of the mesopores between the platelet stacks. A more detailed study, where also small-angle X-ray scattering (SAXS) measurements will be included is planned on the X-fluorohectorite system, with the exchangeable cation X as either Na^+ or Ni^{2+}. The inclusion of SAXS will provide an independent check on the extracted direction-dependent correlation lengths and also give the possibility to study with better time resolution the initial dynamics of water absorption.

The authors would like to thank the machine shop at The Norwegian Institute for Science and Technology (NTNU) for assistance with construction of the sample cell, Jonny Martens for technical assistance, and the staff at the Jeep-II reactor at Institute for Energy Technology (IFE) for providing the cold-moderated neutron beam essential for these experiments.

References

da Silva, G. J., Fossum, J. O., DiMasi, E., Maloy, K. J. & Lutnaes, S. B. (2002). *Phys. Rev. E* **66**, 011303-1–011303-8.
Debye, P., Anderson Jr, H. R. & Brumberger, H. (1957). *J. Appl. Phys.* **28**, 679–683.
Debye, P. & Bueche, A. M. (1949). *J. Appl. Phys.* **20**, 518–525.
DiMasi, E., Fossum, J. O., Gog, T. & Venkataraman, C. (2001). *Phys. Rev. E* **64**, 061704-1–061704-7.
Fossum, J. O. (1999). Unpublished.
Hall, P. L., Mildner, D. F. R. & Borst, R. L. (1983). *Appl. Phys. Lett.* **43**(3), 252–254.
Kaviratna, P. D., Pinnavaia, T. J. & Schroeder, P. A. (1996). *J. Phys. Chem. Solids* **57**, 1897–1906.
Knudsen, K. D., Fossum, J. O., Helgesen, G. & Haakestad, M. W. (2003). Submitted to *Phys. Rev. E* .
Ramsay, J. D. F. (1998). *Adv. Coll. Int. Sci.* **76-77**, 13–37.
Solin, S. A. (1997). *Ann. Rev. Mater. Sci.* **27**, 89–115.
Velde, B. (1992). *Introduction to Clay Minerals.* London: Chapman and Hall.
Wignall, G. D. & Bates, F. S. (1987). *J. Appl. Cryst* **20**, 28–40.

Received 29 August 2002 • Accepted 3 January 2003